Original Article

JOURNAL OF
biomaterials
applications

Journal of Biomaterials Applications
2017, Vol. 31(6) 819–831

DOI: 10.1177/0885328216684652
journals.sagepub.com/home/jba
SAGE

Fabrication of Zn-Sr–doped laser-spinning glass nanofibers with antibacterial properties

María Magdalena Echezarreta-López[1], Trinidad de Miguel[1,2], Félix Quintero[3], Juan Pou[3] and Mariana Landín[1]

Abstract

The morphology and dimensions of bioactive materials are essential attributes to promote tissue culture. Bioactive materials with nanofibrous structure have excellent potential to be used as bone-defect fillers, since they mimic the collagen in the extracellular matrix. On the other hand, bioactive glasses with applications in regenerative medicine may present antibacterial properties, which depend on glass composition, concentration and the microorganisms tested. Likewise, their morphology may influence their antibacterial activity too. In the present work, the laser-spinning technique was used to produce bioactive glass nanofibers of two different compositions: 45S5 Bioglass® and ICIE16M, bioactive glass doped with zinc and strontium. Their antibacterial activity against *Staphylococcus aureus* was tested by culturing them in dynamic conditions. Bacterial growth index profiles during the first days of experiment can be explained by the variations in the pH values of the media. The bactericidal effect of the doped nanofibers at longer times is justified by the release of zinc and strontium ions. Cytotoxicity was analyzed by means of cell viability tests performed with BALB/3T3 cell line.

Keywords

Bioactive glass, laser-spinning, doped nanofiber, antibacterial property, zinc, strontium

Introduction

Biomaterials to be used clinically for bone repair in dentistry, maxillofacial or orthopaedic surgery with antibacterial properties have been growing in interest since they can prevent or treat potential implant-related infections.[1,2] In recent years, a significant number of investigations have shown antibacterial properties in the group of biomaterials known as bioactive glasses (BGs).[3–5]

Degradable glasses in the Na_2O-CaO-SiO_2-P_2O_5 system with high calcium content and a composition close to a ternary eutectic Na_2O-CaO-SiO_2 system[6] can be classified as bioactive materials when they are able to form chemical bonds with bone through the formation of a calcium apatite layer at their surface.[7] BGs exert control over osteoblast genes, regulating osteogenesis and promoting the production of growth factors.[8]

The composition and concentration of the BG together with the microorganism tested are the main factors determining their antibacterial effect.[9] Several authors have also established that the antibacterial properties are conditioned by the manufacturing process and the morphology of the BG.[10] Several strategies can be derived from the literature to increase the antibacterial activity of BGs. The inclusion of metal ions, specially silver,[11] strontium (Sr),[12] zinc (Zn)[13–15] or copper[16] or their combinations have succeeded in reducing microbial contamination. Additionally, these changes in the BG composition can promote variations in other biomaterial features such as their effect on cellular functions, cell metabolism or biological functions, by binding to macromolecules (enzymes or nucleic acids) and/or activating ion channels or secondary signalling.[17,18] Particularly, in the field of bone tissue engineering, there is a great interest for the Sr and Zn

[1]Departamento de Farmacia y Tecnología Farmacéutica, Facultad de Farmacia, Campus Vida, Universidad Santiago de Compostela, Santiago de Compostela 15782, Spain
[2]Departamento de Microbiología y Parasitología, Facultad de Farmacia, Campus Vida, Universidad Santiago de Compostela, Santiago de Compostela, Spain
[3]Applied Physics Department, EE Industrial, University of Vigo, 36310, Spain

Corresponding author:
Juan Pou, University of Vigo EEI, Lagoas-Marcosende, 9. Vigo, Pontevedra 36310, Spain.
Email: jpou@uvigo.es

as they can be cofactors in metabolic processes involving bone and articular tissues formation and immune system functions.[17] Doping BG with Zn or Sr ions has been related to a significant enhancement in the calcium apatite surface layer formation and growth when exposing the material to body fluids, which is necessary for the interaction with the living bone and the material osteointegration.[19,20] Moreover, they have been shown to stimulate osteoblast proliferation and to inhibit osteoclastic bone resorption with potential application in the osteoporosis pathologies.[20,21] Generally, antibacterial ions are included by developing composite materials where the BG and the ions are immersed in a polymer matrix or in a structured system whose antibacterial activity depends on the properties of the polymer matrix.[13,22] Less frequently, ions are incorporated into the BG structure; however, the inclusion of ions such as Zn or Sr has been demonstrated to modify their texture and surface reactivity and, consequently, their solubility and bioactivity.[20,23] In the former cases, ions release is intrinsically related with the bioactivity of biomaterial and therefore with its antibacterial properties.[24] An alternative approach was recently demonstrated: in order to dope with silver a bioactive-glass ceramic scaffold, silver nitrate was added to a glass slurry processed by the sponge replication method.[25] After sintering the silver nitrate was incorporated into the sponge-like scaffold.

On the other hand, nanofibres have a great potential application in regenerative medicine, in defects where load-bearing materials are not needed, since their morphology mimics the natural fibrous structure of collagen in extracellular matrix.[7,26] The first BG nanofibers were produced employing the electrospinning technique.[27] Since that first work, several works explored the bioactive properties of electrospun glasses.[7,28,29] However, to our best knowledge, only the laser-spinning technique has produced amorphous Bioglass 45S5 fibers with micro or nanoscale diameters, apart from a variety of compositions that can be classified as BGs.[30] These nanostructures have several potential applications such as tissue engineering scaffolds, fillers for repairing bone defects or as reinforcing agents in composite implants.

The production of nanofibers by Laser Spinning involves the quick heating and melting up to high temperatures (in the range of 2000 K) of a small volume of the precursor material using a high-power laser.[31] The plate of the precursor material being irradiated is in motion with controlled advance speed in relation to the laser beam, which generates a stable melting front producing a complete or incomplete cut. At the same time, a supersonic gas jet drags the molten material down to the bottom of the cut. The viscous material reaching the bottom edge of the cut forms a pending viscous droplet which is further propelled by the gas jet. Thus, the molten material forms glass fibers as a result of its viscous elongation by the drag force and rapid cooling by the convective heat transfer promoted by the gas jet. The complete process is performed under ambient conditions.

In a different work, Cabal et al.[32] demonstrated the capability of the laser-spinning technique for the production of a bioinert composite consisting of metallic silver nanoparticles embedded in silicate glass nanofibers. They also reported a long-lasting antibacterial activity of those fibers, thanks to the dispersed presence of silver nanoparticles in the surface and into the volume of the nanofibers.

The aim of the present study is to highlight the potential of Zn and Sr –doped BG nanofibers produced by laser-spinning as a new material that can combine the well-known bone-regenerating properties of BGs with the antibacterial properties of the released ions. The antibacterial properties of laser-spinning nanofibers based on the 45S5 Bioglass® composition are evaluated and compared to previous works. Additionally, cytotoxicity analyses are presented in order to assess and compare cell viability under the ion release produced by doped and undoped glass fibers.

Materials and methods

Glass nanofibers preparation

Two types of glass nanofibers were produced by the laser-spinning technique developed by Quintero and co-workers.[31] The precursor materials employed to produce the glass fibers were glass plates with the following compositions: M1/45, with the same nominal composition of 45S5 Bioglass® developed by Hench and co-workers[6] and ICIE16M[33,34] a BG with a modified composition of Bioglass 45S5, were sodium was partially substituted for K_2O, MgO, ZnO and SrO.

Table 1 shows the nominal compositions of both glasses. Several plates of each glass composition were produced by means of the conventional method of melting in a platinum crucible and casting into graphite moulds. These plates were employed as precursor materials in the laser-spinning process. A high-power CO_2 laser (DC 035, Rofin-Sinar, Germany) was

Table 1. Composition of laser-spinning glass nanofibers (mol %).

Name	SiO_2	CaO	Na_2O	K_2O	P_2O_5	MgO	SrO	ZnO
ICIE16M	49.46	27.27	6.60	6.60	1.07	3.00	3.00	3.00
M1/45	46.1	26.9	24.4	–	2.6	–	–	–

operated in continuous mode emitting 2.5 kW of laser radiation, which was focused over the glass plate to melt a small volume of it through its full thickness. Simultaneously, a supersonic air jet was used to blow the molten material provoking the elongation and cooling of viscous filaments which eventually will form the glass fibers. This method allows the incorporation of Zn and Sr ions from suitable precursors. Glass nanofibers were pretreated by immersion in water milliQ for 1 min, filtrated and dried at 50°C for 24 h before the study.

Glass nanofibers characterization

Crystal diffraction measurements were carried out to determine structural characteristics of laser-spinning glass nanofibers and the formation of phosphate structures, like apatite on the surface of nanofibers collected after antibacterial studies. Crystallinity of nanofibers was analyzed by X-ray diffraction (XRD) patterns collected using a Philips diffractometer (PW1710 Corp. Netherland) operating at 40 kV and 30 mA). The X-ray were obtained from a Cu-sealed tube and the radiation was monochromatized with a graphite monochromator (λ ($K_{\alpha 1}$) = 1.5406 Å). The times and ranges of measurement were adjusted to conditions where the main peaks of calcite and apatite phases could be distinguished. Thus, data collection was carried out in the angular range of 10–40° with a pitch of 0.02° and accumulation time 10 s. Samples were rotated during the measurements to obtain the optimal peak profiles for analysis and to minimize the effects of preferred orientation. A sample holder-oriented crystal Si was used. On the other hand, the density of laser-spinning glass nanofibers was determined in triplicate using a helium-air pycnometer Quantacrome (Mod. PY2, USA).

Cytotoxicity analysis

The in vitro cytotoxicity tests for glass nanofibers were performed on extracts prepared by elution of the samples (75 mg/mL) in Dulbecco's modified Eagle's medium (DMEM) (GIBCOTM), supplemented with 10% fetal bovine serum (FBS) and 1% gentamicin in duplicate at 37 °C for 48 h. Cell viability tests were performed with BALB/3T3 cell line (CCL 163, ATCC, USA), according to the 10993-5 protocol of the International Standardization Organization (ISO). A cell suspension of 2×10^4 cells/well in 200 µL of DMEM was added into a 96-well plate and allowed to grow. After 48 h, different concentrations of ICIE16M and 45S5 glass nanofibers extracts (0.5, 1 and 2%) were added to the cells and the plate was incubated at 37°C in a humidified atmosphere with 5% CO_2. A control (cells without glass nanofibers extracts) was treated in the same way. The 3-(4, 5-dimethylthiazol-2-yl)-2, 5-diphenyl tetrazolium bromide (MTT) assay was used in this study to measure cell viability. MTT assay measures intracellular mitochondrial activity of the cells, which involves reduction of MTT by intracellular dehydrogenases of viable cells to blue formazan. Cells survival was evaluated through the measurement of absorbance at 550 nm using a microplate reader (BIORAD Model 680, Hercules, CA USA).

Each experiment was carried out in duplicate. In order to calculate the reduction of viability compared to the control sample (blank), the following calculations were performed according to protocol "MTT cytotoxicity test" included in the standard ISO 10993-5

$$Viab.\ \% = \frac{100 \times OD_{550e}}{OD_{550b}}$$

where OD_{550e} is the mean value of the measured optical density of the 100% extract of the test sample; OD_{550b} is the mean value of the measured optical density of the blanks. The lower the viab % value, the higher the cytotoxic potential of the test item is. If the viability is reduced to <70% of the blank, it has a cytotoxic potential.

In order to study the potential non-cellular reduction of MTT by metal oxides (Zn and Sr oxides) in the doped nanofibres,[35] that can induce the reduction of MTT dye molecules to formazan crystals leading to false positive results, an additional control (ICIE16M nanofibres + MTT, without cells) was included.

Antibacterial properties study

Microbiological studies were carried out with laser-spinning glass nanofibers at different concentrations (5, 25 and 75 mg/mL) using *Staphylococcus aureus*, *a* Gram-positive bacteria. *S. aureus* (CECT 240) was incubated in Tryptic Soy Broth (TSB) medium pH 7.3 to reach a density of about 10^6 cells/mL. Then 100 µL of this culture were inoculated in an eppendorff tube containing 900 µL of fresh TSB medium together with the previously sterilized nanofiber. An eppendorff tube without nanofibers was used as control. The eppendorff tubes were sealed with Parafilm® and incubated in an orbital shaker at 200 r/min and 37°C for 4 days. An aliquot of 50 µL of this culture was taken every 24 h; 10 µL were used to check bacterial presence using scanning electron microscopy (SEM) and the rest to perform serial dilutions. In all, 50 µL of dilutions 10^{-4}, 10^{-5} and 10^{-6} were plated in triplicate on TSA medium and incubated at 37°C for 24 h. The number of colonies was calculated by averaging the three values obtained by counting the number of colonies for the

three plates corresponding to each concentration of the fibers and time of culture. Previously, the three different dilutions were inspected to select the most feasible one for the recount of colonies; accordingly, all plates with the same dilution were assessed. After counting plate colonies, a bacterial growth index was established according to the following parameters: Level 4: >>> 300 colonies (countless); Level 3: > 300 colonies (countable); Level 2: 30–300 colonies; Level 1: 0–30 colonies; Level 0: no colonies. The variations of pH medium were measured using a pH Meter (GLP22, Crison, Spain) at each time interval.

Additionally, samples of the TBS medium were collected from the experiment carried out with doped glass nanofibers (ICIE16M at 75 mg/mL) and the concentration of released Zn and Sr ions measured up to 7 days of incubation by Optical Emission Spectroscopy Inductive Coupled Plasma Spectroscopy (ICP-OES) using a Perkin-Elmer Optima 3300DV system (Norwalk, USA).

Attenuated total reflection-Fourier transform infrared spectroscopy

The structural glass nanofibers characteristics were analyzed before and after the antibacterial studies by attenuated total reflection-Fourier transform infrared spectroscopy (ATR-FTIR). The samples were washed twice with sterile MilliQ and centrifuged at 8000 r/min during 2 min (Microfuge®22 R Centrifuge Beckman Coulter™). ATR-FTIR analysis was carried out in a 670IR Varian (USA) spectrometer equipped with a Gladi-ATR single-reflection spectrometer, Pike Technologies (Madison, EEUU). Spectra were recorded on an average of 256 scans at a resolution of 4 cm^{-1} in the 400–4000 cm^{-1} range.

Electron microscopy analysis

Morphology and surface characteristics of gold-coated laser-spinning glass nanofibers were analyzed before and after the antibacterial study using SEM (Leo 435VP, Cambridge, UK). ICIE16M nanofibers were collected after the incubation with *S aureus*, fixed according to Santhana and co-workers[36] and analyzed using a transmission electron microscopy (TEM; JEOL JEM-1011, Tokyo, Japan) in order to evaluate their physical interaction with bacteria.

One representative sample was analyzed in order to measure the diameters of the fibers using a Field Emission Scanning Electron Microscope (FESEM), Jeol JSM 6700. The fibers were dried and analyzed without coating. In order to achieve a representative sampling to perform a correct statistical analysis, we made 22 randomly located micrographs: two micrographs with magnification of × 500 – to measure thicker fibers, and 20 at × 5000 – so that thinner fibers can be measured, since the area scanned at × 500 is 10 times the area scanned at × 5000. The fiber diameters were measured from the micrographs using image analysis software.

Results

Glass nanofibers characterization

A cotton-like mesh of nanofibers was obtained for both glass compositions. SEM micrographs (Figure 1) show an overall view of their appearance. The fibers have a uniform well-defined cylindrical morphology (diameters ranging between tens of nanometers and 5 μm) and they form a disordered intertwined net of fully dense, solid and completely separated nanofibers.

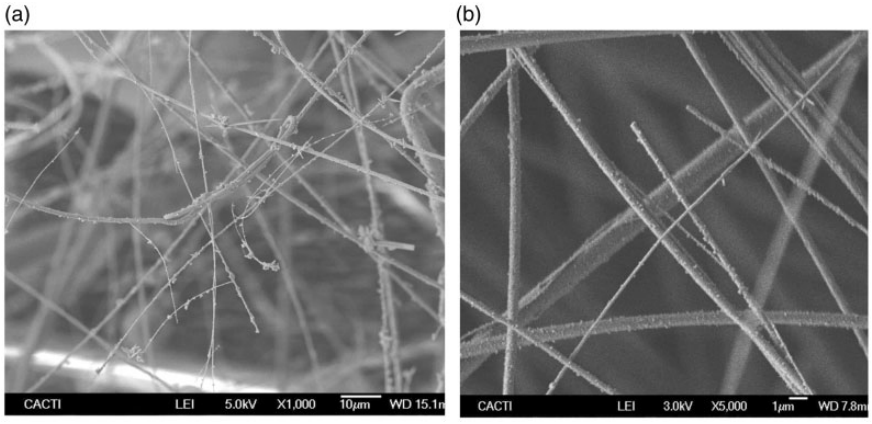

Figure 1. SEM micrographs of laser-spinning glass nanofibers. (a) Typical appearance of as-produced ICIE16M fibers and (b) detail of M1/45 Bioglass nanofibers.

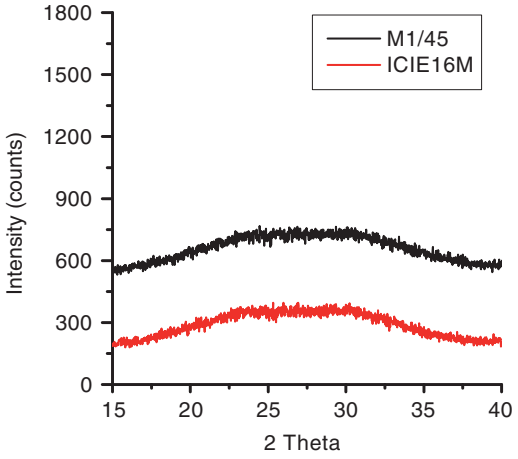

Figure 2. XRD patterns of laser-spinning glass nanofibers.

Some spherical particles mixed with the nanofibers can also be observed. Their formation is related to the ratio of viscosity to surface tension of the viscous filament during its elongation and cooling. At some points of the molten volume, the surface tension promotes the break-up of the fluid filament into droplets and, hence, spheroidal particles are formed.[31]

XRD patterns show that both, M1/45 and ICIE16M glass nanofibers, obtained by the laser-spinning technique are amorphous (Figure 2). The incorporation of ion modifiers (Mg^{2+}, Zn^{2+} and Sr^{2+}) does not affect the crystalline structure.

The evaluation of density measurements, which have been used as a method to make conclusions on the silicate glasses microstructure by several authors,[37,38] indicates differences between these complex glasses as a function of their composition, the density being by the helium picnometry of $2.0 \pm 0.001\ g{\cdot}cm^{-3}$ and $2.3 \pm 0.0\ g{\cdot}cm^{-3}$ for M1/45 and ICIE16M (doped glass nanofibers), respectively. The higher density of doped nanofibers is caused by the inclusion of magnesium, Sr and Zn ions in their composition. The volume change in the structural units by introducing those ions justify the differences in density between nanofibers and therefore in their microstructure and presumably in their properties. The absolute values of density seem to be significantly lower than those predicted according to previous studies;[37,38] these differences may be due to the morphology of the nanofibers with high surface area which may adsorb a relevant quantity of water vapor.

One representative sample was selected to measure the diameters distribution of the fibers using the FESEM. A number of more than 250 fibers were measured using the image analysis software and the results are presented in the histogram shown in Figure 3, representing the relative frequency of occurrence as a function of fiber diameters in micrometers.

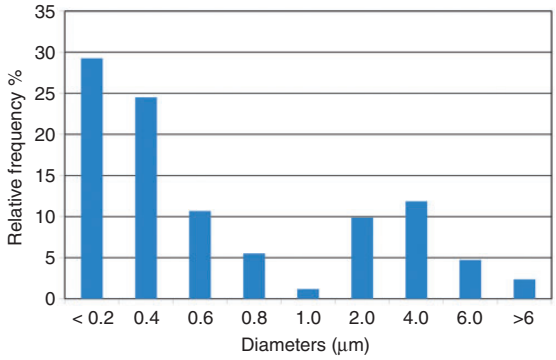

Figure 3. Histogram representing the distribution of diameters of the fibers of a representative sample.

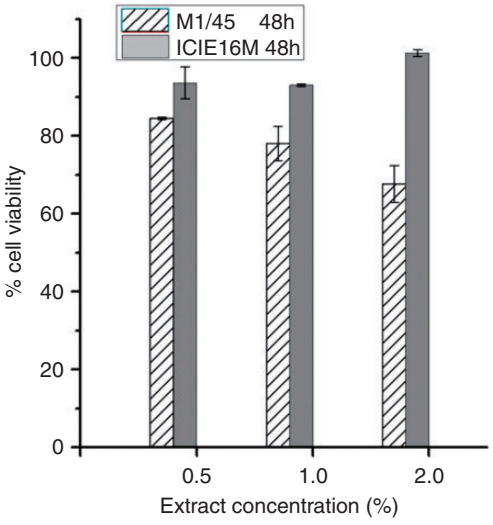

Figure 4. Results of cytotoxicity tests of M1/45 and ICIE16M laser spinning glass nanofibers after 48 h.

Cytotoxicity results

Cytotoxicity of the glass nanofibers was screened using fibroblast (BALB/3T3) cell line. Figure 4 shows the results of the cell viability percentage after incubation of cells with extracts of both M1/45 and ICIE16M glass nanofibers for 48 h. The cell viability obtained is higher than 90% for ICIE16M, but it is lower for the M1/45 glass nanofibers, and it decreases with extract concentration. This result can be justified by the rapid dissolution of M1/45 glass nanofibers, which quickly releases alkali ions to the medium. Results for the (ICIE16M + MTT without cells) control demonstrate a reduction effect of metal ions by themselves, proportional to the concentration of nanofibers in the experiment. Therefore, there is a bias promoted by the metal oxides reduction up to 30% for the highest concentration.

Antibacterial studies

The antibacterial properties of laser-spinning glass nanofibers, M1/45 and doped nanofibers ICIE16M were evaluated. For this purpose *S aureus* and glass nanofibers were incubated for 4 days at 37°C with stirring. The bacterial growth indexes were calculated by averaging the number of colonies obtained from the three replicates of each sample. Statistical dispersion among three values of each sample was not relevant for the calculation of the growth index. The profiles of bacterial growth versus time for experiments carried out with the two varieties of nanofibers at different concentrations are shown in Figure 5.

Antibacterial behaviour of the nanofibers differs with regard to their composition. Only doped nanofibers (ICIE16M) at the highest concentration promoted inhibition of bacterial growth at a value of 2 indicating a bactericidal effect after 4 days of incubation. ICIE16M nanofibers at lower concentration than 75 mg/mL and M1/45 fibers show a bacteriostatic effect. Moreover, no effect can be observed when using M1/45 fibers at lower concentration before 2 days.

Those results can be partially justified by the variations of media pH during the experiment as a consequence of alkaline ions released from the fibers. In general, as a result of the nanofibers dissolution, an alkalization of the medium occurs. As it can be seen in Figure 6, the presence of nanofibers, both M1/45 and ICIE16M, in a concentration over 5 mg/mL gives a significant increase in the pH of the medium, greater than 8.0 for concentrations of 25 mg/mL or even 9.5 when using bioglass nanofibers (M1/45) at a concentration of 75 mg/mL. These results indicate that the bioglass nanofibers dissolution increases the pH of the medium faster than doped nanofibers (ICIE16M) at 75 mg/mL, affecting the survival of bacteria at the

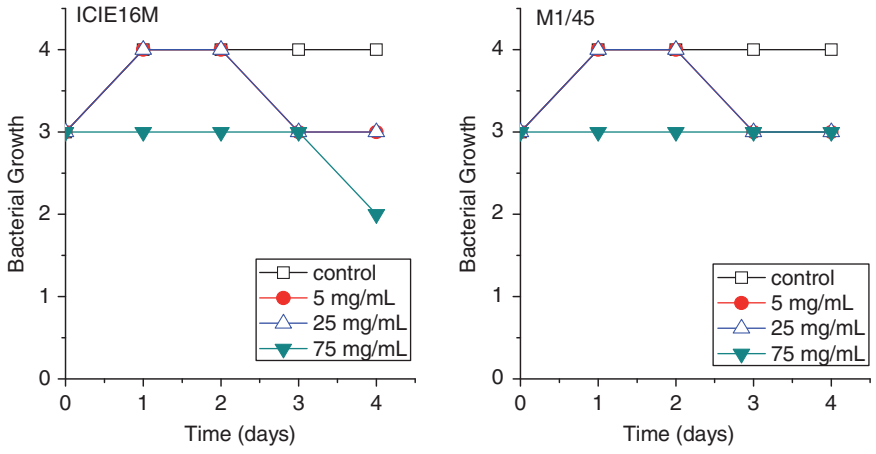

Figure 5. Bacterial growth index versus time of cultures of *S. aureus* in the presence of both, M1/45 and ICIE16M doped laser-spinning nanofibers at different concentrations.

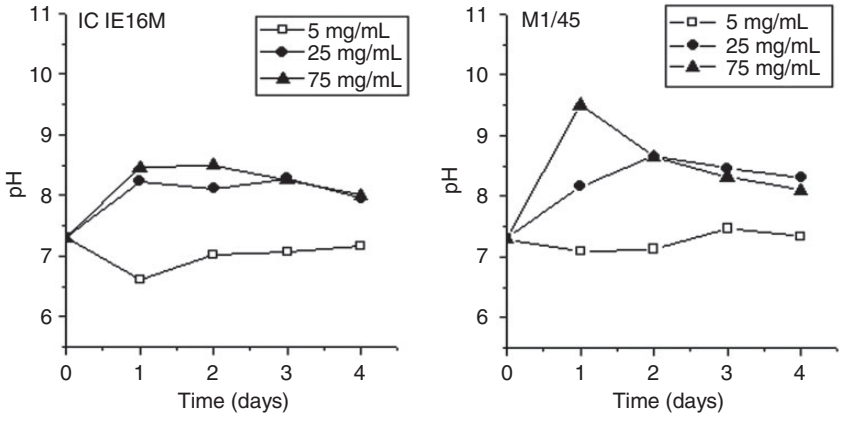

Figure 6. pH medium at different concentration of laser spinning glass nanofibers.

shorter periods of times. The increase in the pH is not maintained within the time range as the pH decreases after the second day of culture, especially for the bioglass nanofibers. The increase in the bactericidal effect of the doped nanofibers after 2 days of culture may be well justified by the delayed release of metal ions.

The partial dissolution of the nanofibers and, therefore, the structural changes and surface modifications were investigated by FTIR, XRD and SEM by comparing laser-spinning glass nanofibers before and after the antibacterial studies.

Figure 7 shows the evolution of Zn and Sr concentration with the time for the antibacterial experiment carried out with ICIE16M fibers at a concentration of 75 mg/mL for 7 days. As it can be seen, the concentrations of both Zn and Sr ions increase significantly after the second day of incubation, in agreement with the beginning of the observed antibacterial effect of those nanofibers.

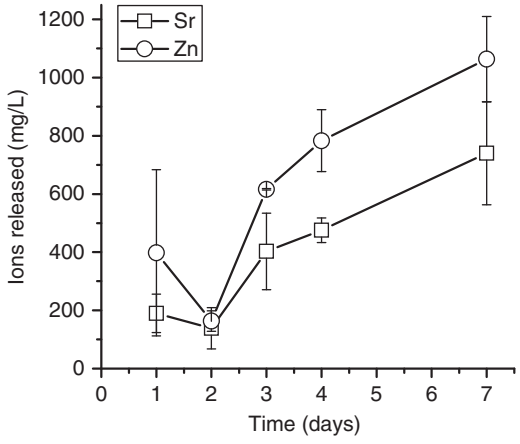

Figure 7. Evolution of metal ions released concentrations in TSB medium at 37°C for 7 days.

Metal ion concentrations in the TSB medium achieve values of 1.0 mg/mL and 0.65 mg/mL at 7 days for Zn and Sr, respectively, which can be responsible of the antibacterial activity.

Figure 8 shows the FTIR spectra of two laser-spinning nanofibers before and after the antibacterial studies. Both M1/45 and ICIE16M nanofibers present, as supplied, the characteristic absorption bands of SiO_4 units at 1024, 900 and 450 cm^{-1} corresponding to the Si-O-Si stretching mode, Si-O and Si-O-Si bending mode, respectively, which is in agreement with previous reports.[39,40] The incorporation of ion modifiers Zn, Sr and Mg into the original SiO_4 network does not change the characteristic bands of SiO_4 units.

After their immersion into the culture medium solution for 4 days, several modifications can be observed as a consequence of their different dissolution process. A non-bridging oxygen (NBO) band at 920 cm^{-1} is maintained for the doped nanofibers (ICIE16M) while in the bioactive nanofibers (M1/45) it disappears. Simultaneously, new bands at 560 and 600 cm^{-1} can be observed for M1/45 spectrum (Figure 8), which can be associated to the deposition of PO_4^{3-} groups as pointed out by other authors.[20]

The small sharp features at 715 and 870 cm^{-1} together with the new band at 1422 cm^{-1} exhibited by the FTIR spectra of the M1/45 nanofibers after incubation in the culture medium can be also associated to the formation of carbonated hydroxyapatite (HCA) layers on the surface of the material as a consequence of its bioactive nature.[20] These results confirm the modifications in their surface composition and point out the partial dissolution of the bioactive nanofibers

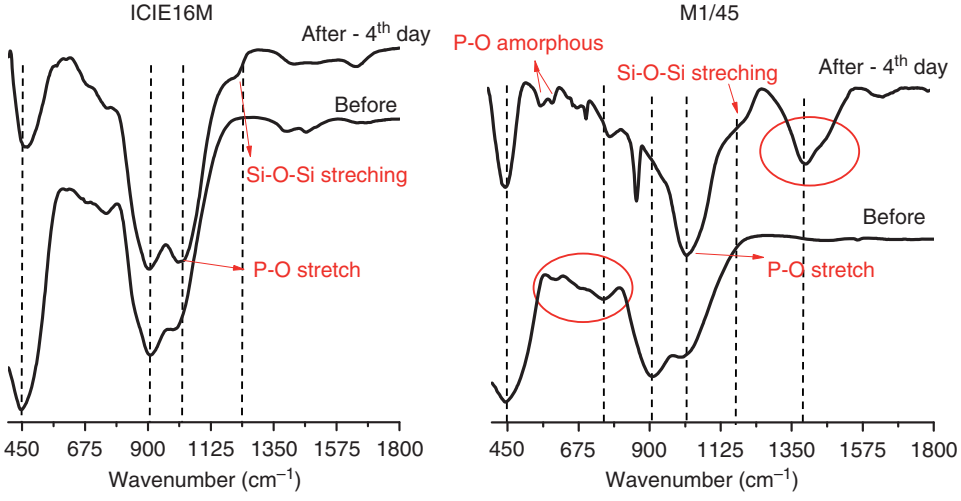

Figure 8. FTIR spectra of glass nanofibers before and after four days in presence of *S aureus* growing in TSB medium.

during microbiological studies. On the contrary, those modifications do not appear at the ICIE16M spectrum, suggesting that any or poorly crystalline apatite has been formed on doped nanofibers surface after 4 days of incubation with the bacteria.

The morphology and surface structure of the nanofibers recovered from the antibacterial studies were also analyzed by SEM, EDX and XRD, which allowed a semi-quantitative characterization of the samples surface chemistry and their structural surface modifications. EDX results (not shown) revealed Mg, Zn and Sr elements at the surface of ICIE16M nanofibers after incubation time and in TSB medium.

In agreement with FTIR results, XRD patterns of nanofibers after 4 days of incubation in culture medium indicate the formation of a crystalline phase of calcite and hydroxyapatite on the surface of the bioglass nanofibers (M1/45). Moreover, the higher the concentration of the nanofibers, the stronger the crystalline modifications are. Structural changes cannot be observed on the surface of the doped nanofibers (Figure 9) confirming the differences in its dissolution process.

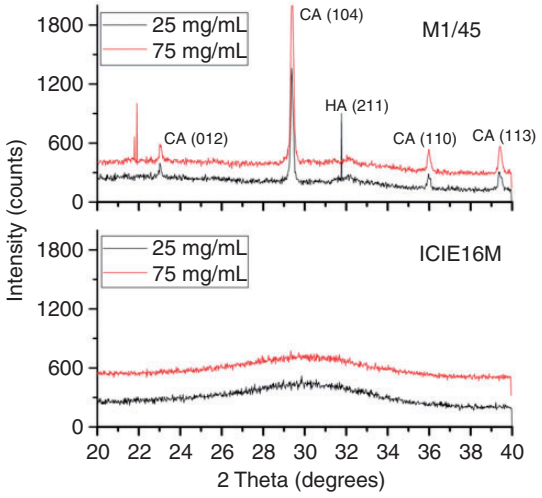

Figure 9. XRD patterns of glass nanofibers after four days of incubation with *S. aureus* in TSB medium. The peaks are very precisely assigned to the indexed crystallographic planes of calcite (CA, JCPDS-ICDD ref.:005-0586) and hydroxyapatite (HA, JCPDS-ICDD ref.:09-0432).

The antibacterial effect of the BGs may be intensified by physical interactions between bacteria and debris generated during their process of dissolution as it has been previously described.[41] In order to evaluate potential physical interactions between bacteria and nanofibers, *S aureus* after 4 days of culture in the presence of ICIE16M nanofibers (75 mg/mL) was visualized by TEM. Figure 10 presents two areas of the culture.

Discussion

BGs based on different combinations of alkaline earth oxides have demonstrated an excellent biocompatibility, osteoconductivity and osteostimulation. Those properties make them suitable candidates as implant materials for dental and orthopedic surgery.[42] In the last few years, different authors have demonstrated that BGs show antibacterial activity on selected microbial species depending on their composition and concentration.[5,9,43] On this basis, the design of BGs with antibacterial properties can be an interesting approach to prevent or treat potential implant-related infections.[44]

The inclusion of metal ions, like Sr or Zn, in BG systems have been proposed as an interesting strategy to obtain implants with antibacterial activity.[12,13] Those ions not only are toxic for a broad spectrum of microorganisms but they promote variations in other cellular functions, enhancing the interaction with the living bone and promoting the implant osteointegration.[19,20] On the other hand, by substituting Sr for Ca, glass degradation and apatite formation can be increased.[20] At the same time, Sr not only stimulates increased osteoblast metabolic activity and inhibits osteoclast differentiation and resorption but also promotes osteoblast proliferation and alkaline phosphatase activity.[45]

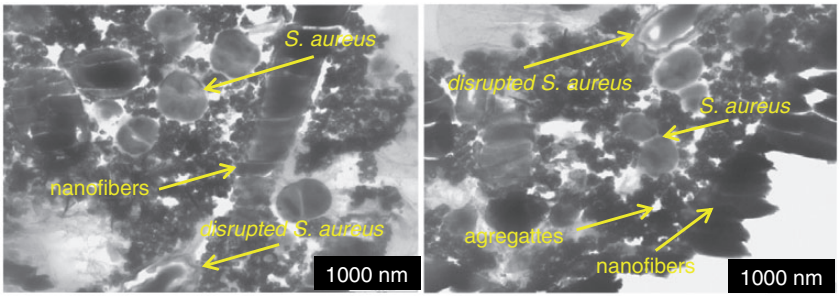

Figure 10. TEM images of four days incubation cultures of *S aureus* in TSB with ICIE16M glass nanofibers (75 mg/mL).

In this work, two batches of laser-spinning glass nanofibers, M1/45 with same nominal composition as the original 45S5 Bioglass® developed by Hench and co-workers and ICIE16M doped with magnesium, Sr and Zn as ions modifiers, were produced. The introduction of modifiers in doped nanofibers is carried out as a result of reducing Na and P ion concentrations but maintaining the calcium ion content because Ca^{+2} has been related to the antibacterial activity of BGs.[9]

The laser-spinning technique allowed the incorporation of required ions using precursors of different melt-derived compositions. The nanofibers obtained for both compositions are amorphous. They have a cylindrical morphology and appear fully dense, solid and completely separate, forming an easy-to-handle cotton-like mesh.

The incorporation of ion modifiers (Mg^{2+}, Zn^{2+} and Sr^{2+}) does not affect the crystallinity but promotes some changes in the density of materials, which have been related to bioactive properties of BG[20,38,46] and, therefore, to their antibacterial properties. The bioactive properties of BGs are strongly related to the alkali metal content and their contribution into the structure, making it possible to tailor physical and biological BG functions modifying alkali metal composition.[38]

The backbone of the glass silicate structure is an SiO_4 tetrahedral continuous network connected by their corners. Alkali and alkaline earth oxides modify this network structure, reducing the degree of connectivity in the network by replacing bridging oxygens (BO) with NBOs. Network formers give a structure, with bridging and NBOs, while the mobile ions occupy the free spaces. Network modifiers disrupt the glass structure. The structural modifications of SiO_4 units produced by the incorporation of Mg, Zn and Sr ions modify the local Ca environment, and as a consequence, its dissolution process and the biological activities involved.

The replacement of Na and P ions by Mg, Sr or Zn ions for doped nanofibers should endorse the change in the coordination structure and their cross-linking. Depending on the nature and composition of the glass, the oxides MgO, ZnO and SrO can enter the structure as a network modifier and/or a network former, behaving like the alkali oxides of glass.[37] The differences in densities recorded for the two laser-spinning glass nanofibers indicate that the inclusion of metal ions into the doped nanofibers should promote a more closed structure, limiting the access of the medium and, therefore, slowing down the dissolution of the nanofibers and, consequently, affecting their bioactivity. The decrease in the release rate of potential toxic ions could have an impact on the effectiveness of the nanofibers against bacteria.

The in vitro cytotoxicity studies, investigated through MTT tests (Figure 4), show that Bioglass® nanofibers (M1/45) promote lower percentages of cell viability in comparison with the doped glass nanofibers (ICIE16M). Those differences can be justified by the reduction effect of metal ions that magnifies MTT result (up to 30% for maximum extract concentration). Even considering this distorsion, neither the M1/45 nor the ICIE16M glass nanofibers extracts at any concentration show high toxicity for fibroblast (B 323 ALB/3T3) cells 48 h.

S aureus is a Gram-positive bacteria commonly used to study antibacterial properties of BGs because it is frequently involved in the infection problems derived from dental and orthopaedic surgery, promoting implant failure.[1] From our results, we can deduce that BG concentration and composition have a significant effect on antibacterial behavior of both bioactive and doped nanofibers (Figure 5) as it has been previously described. Those differences can be justified by variations in the amount and rate of ions released as is pointed out by the pH evolution during the experiment (Figure 6). The alkalinisation of the media by dissolution of the BG has been stated as being mainly responsible of antibacterial properties of 45S5 BG[9] either when the bioglass was tested directly[10] or included in composites[47] and in scaffolds.[48] The optimal pH values to growth of *S aureus* range between 7.0 and 7.5. After the first day of incubation, the pH of the medium when the bioactive nanofibers concentration are over 5 mg/mL is higher than the optimum, explaining the antibacterial effect promoted after the second day of the experiment. The increase in nanofibers concentration reduces the lag period in the antibacterial effectiveness. These results are in agreement with Rivadeneira and co-workers[49] who have demonstrated the antibacterial activity of biocomposite films including 45S5 bioglass microparticles against staphylococci.

Secondly, the nanometric morphology of these BGs has a great influence on its antibacterial properties. Waltimo et al.[10] suggest that increased specific surface area of nanometric BG promotes greater ion release and consequently displays a stronger antibacterial effect. These authors justified the increase of antibacterial effect also with the higher pH that is obtained in comparison with conventional BG 45S5 (Perioglass™). The local bacterial effect of conventional 45S5 bioglass particle has been attributed to bioglass debris producing a mechanical erosion on the bacterial surface of *S aureus*, *S epidermidis* and *E coli*;[41] however, this effect was not observed in the present work.

The degradation, ions release and hydroxyapatite formation of 45S5 Bioglass nanofibers produced using the same method than the present work was analyzed across 10 days of immersion in simulated body fluid

(SBF) and reported in a previous work by Quintero et al.[30] Those results revealed that the silica network of the 45S5 Bioglass nanofibers undergoes almost complete dissolution in 48 h, together with the consequent high release of Ca ions. Subsequently, after 48 h of immersion, the Ca ion concentration started to decrease slowly due to the precipitation of calcium phosphate on the surface of the fibers. This ion release kinetics is in great accordance with the rapid increase in pH of the medium observed in the present work during the first 2 days, followed by a slower pH reduction that agrees with the continuous antibacterial effect of these fibers.

Doped nanofibers with concentration over 5 mg/mL also promote an alkalinisation of the medium leading to a bactericidal effect similar to that of the bioactive nanofibers during the first 2 days of experiment. However, the reduction in the growth index afterwards at a highest concentration of nanofibers cannot be simply explained by the variations in pH but by the slow release of metal ions, which are toxic for bacteria.[12,50]

The introduction of metal ions modifies the connectivity of the glass-forming network, alters the local environment of active Ca^{2+} and modifies the kinetics of the dissolution process and therefore the evolution of the antibacterial properties of this material. The release profiles of Zn^{+2} and Sr^{+2} ions (Figure 7) from the doped nanofibers at 75 mg/mL show a progressive increase of toxin for bacteria substances during the experiment, particularly after the second day of experiment, in agreement with the corresponding growth index profile. The presence of toxic effect for bacteria substances justifies the antibacterial effect observed after the second day. The effect of several metal ions and particularly Zn on bacteria at cellular and biochemical level has recently been studied by several authors.[51,52] Metal ions contact promotes variable resistance in *S aureus* bacteria by acting as mutagenic and promoting changes both in biochemical and protein profiles. In comparison with other metal ions as Cu^{+2} or Ag^{+}, *S aureus* bacteria are more tolerant to Zn ions. This fact has been related to the presence of an efflux mechanism together with the ability of the cells of forming an effective shield on the bacterial surfaces. The lag period of 2 days in the antibacterial activity can be related to the ability of the bacteria strains to develop resistances against heavy metals[53] or to necessary contact time to achieve critical concentration of metal ions to promote toxicity.[54]

The toxic effect of Zn ions is bacteria-dependent.[55,56] It has been attributed to the lipid peroxidation of proteins sited at some bacterial cell membranes.[54] The accumulative process of Zn ions released from the nanofibers on the bacteria membrane must affect their metabolism.[56,57]

In addition, it has been described that Sr ions in the range of 0.01 mg/mL–0.2 mg/mL in the culture medium have an effect on the proliferation of bacteria, but also enhance the formation of bone.[12] The developed doped nanofibers are able to release Sr ions in adequate concentration suggesting its utility as a potential antibacterial biomaterial that promotes the formation of bone.

The results obtained on the antibacterial properties of the two laser-spinning nanofibers glasses studied are in accordance with the relationships between BG characteristic and their antibacterial behavior that are established by artificial intelligences tools.[9]

The bioactivity of M1/45 nanofibers is pointed out by the FTIR and XRD results. When the nanofibers enter into contact with the culture medium, physicochemical reactions between the glass and the biological solution lead to the formation of hydroxyapatite layer on its surface. The first step is a rapid exchange of cationic ions between the glass and the solution, followed by dissolution of the silica and the formations of silanol groups. The polycondensation reactions of silanols on the surface generates a silica-rich layer which acts as a nucleus for the formation of Ca-P layer. The formation of stable apatite is closely dependent on the structural properties of the materials and also on its composition.[58] These physicochemical reactions were clearly observed for the same 45S5 Bioglass nanofibers immersed in SBF and reported in a previous work.[30] The rapid degradation of the silica network of the fibers followed by amorphous calcium phosphate precipitation was demonstrated, resulting in the formation of hollow nanotubes of amorphous calcium phosphate in 48 h. This precipitate started to crystallize after the fifth day of immersion, and formed a well-developed structure of hydroxyapatite nanocrystals after 10 days.[30] Similarly, in the present work, the formation of a crystalline phase on the M1/45 nanofibers samples after being in contact with the culture medium is clearly detectable by modification in its XRD pattern. However, in the present case, the formation of calcite on M1/45 glass nanofibers is more evident than hydroxyapatite. This difference could be related to the presence of organic compounds in the culture medium (TSB in the present work) that may react with the calcium ions released by the fibers.

Those surface modifications that cannot be detected for the ICIE16M nanofibers may be provoked by the presence of Mg in their composition which has been related to the inhibition of the formation of calcium phosphate microdomains[59] and the decrease in bioactivity.[46] Furthermore, Zn is known to retard the nucleation rate of apatite formation during the initial phase of SBF immersion while it also inhibits the transformation of amorphous apatite into crystalline carbonated hydroxyapatite.[23,60] The lack of change in the

XRD pattern (Figure 9) and the persistence of the NBO band at 920 cm^{-1} in the FTIR spectra (Figure 8) of the ICIE16M nanofibers after four days of immersion in TSB medium are evidences of the slower degradation rate of these fibers in comparison with 45S5 Bioglass, and is in good accordance with the prolonged release rate of Zn and Sr ions observed (Figure 7).

TEM micrographs of ICIE16M nanofibers (Figure 10) do not show the mechanical or physical effect of nanofibers on the bacteria which has been demonstrated for other nanofibers compositions.[61] The increase in the effectiveness against *S aureus* after the third day of culture (Figure 5) can be attributed to the toxic effect of Zn and Sr ions on bacterial biological mechanisms for the 75 mg/mL concentration. At this concentration, some cell walls (Figure 10) seem damaged after 4 days of culture, suggesting a toxic effect derived from physicochemical changes in bacterial environment, pH or potential interfacial variations promoted by the presence of the doped nanofibers.

Conclusions

In summary, laser-spinning technique allowed the production of amorphous fully dense and solid nanofibers of cylindrical morphology which generated an easy-to-handle cotton-like mesh. By their composition they can be classified as BG (M1/45) and Zn-, Sr-doped nanofibers (ICIE16M). Both nanofibers demonstrated a significant antibacterial effect as a consequence of the increase in the pH of the culture medium due to their partial dissolution and the release of alkaline ions. Conversely, the *in vitro* cytotoxicity tests, performed according to standard ISO-10993-5, proved that they do not show high toxicity for fibroblasts (B 323 ALB/3T3) cells after 48 h. The dissolution, particularly important for M1/45, is demonstrated by the formation of a crystalline layer of calcium phosphate on its surface, detectable by XRD and the FTIR.

Moreover, the inclusion of ions in the nanofibers structure leads to the modification in their dissolution kinetics. Doped nanofibers show additional bactericidal effect for longer times that can be justified by the release of Zn and Sr ions.

Laser-spinning technology is a promising technique to produce nanofibers of adequate composition with antibacterial properties useful in dentistry, maxillofacial or orthopaedic surgery.

Acknowledgement

Authors thank Ms J Menis for her help in the correction of the English version of the manuscript. MMEL thanks the Galician Government, Xunta de Galicia, for its financial support by INCITE_Isabel Barreto Program. Authors also thank Prof Robert Hill and Prof Julian Jones for their fruitful discussions and for introducing them into the use of Zn and Sr in bioactive glasses.

Declaration of conflicting interests

The author(s) declared no potential conflicts of interest with respect to the research, authorship, and/or publication of this article.

Funding

The author(s) disclosed receipt of the following financial support for the research, authorship, and/or publication of this article: This work was supported by the POCTEP 0330IBEROMARE1P project, FEDER, UE and by Xunta de Galicia (CN2012/292).

References

1. Campoccia D, Montanaro L and Arciola CR. The significance of infection related to orthopedic devices and issues of antibiotic resistance. *Biomaterials* 2006; 27: 2331–2339.
2. Busscher HJ, van der Mei HC, Subbiahdoss G, et al. Biomaterial-associated infection: locating the finish line in the race for the surface. *Sci Transl Med* 2012; 4: 153rv10.
3. Stoor P, Söderling E and Salonen JI. Antibacterial effects of a bioactive glass paste on oral microorganisms. *Acta Odontol Scand* 1998; 56: 161–165.
4. Munukka E, Leppäranta O, Korkeamäki M, et al. Bactericidal effects of bioactive glasses on clinically important aerobic bacteria. *J Mater Sci Mater Med* 2008; 19: 27–32.
5. Mortazavi V, Nahrkhalaji MM, Fathi MH, et al. Antibacterial effects of sol-gel-derived bioactive glass nanoparticle on aerobic bacteria. *J Biomed Mater Res Part A* 2010; 94: 160–168.
6. Hench LL. The story of bioglass®. *J Mater Sci Mater Med* 2006; 17: 967–978.
7. Jones JR. Review of bioactive glass: from hench to hybrids. *Acta Biomaterialia* 2013; 9: 4457–4486.
8. Rahaman MN, Day DE, Sonny Bal B, et al. Bioactive glass in tissue engineering. *Acta Biomater* 2011; 7: 2355–2373.
9. Echezarreta-López MM and Landin M. Using machine learning for improving knowledge on antibacterial effect of bioactive glass. *Int J Pharm* 2013; 453: 641–647.
10. Waltimo T, Brunner TJ, Vollenweider M, et al. Antimicrobial effect of nanometric bioactive glass 45S5. *J Dent Res* 2007; 86: 754–757.
11. Bellantone M, Williams HD and Hench LL. Broad-spectrum bactericidal activity of Ag_2O-doped bioactive glass. *Antimicrob Agents Chemother* 2002; 46: 1940–1945.
12. Brauer DS, Karpukhina N, Kedia G, et al. Bactericidal strontium-releasing injectable bone cements based on bioactive glasses. *J R Soc Interface* 2013; 10: 20120647.
13. Boyd D, Li H, Tanner DA, et al. The antibacterial effects of zinc ion migration from zinc-based glass polyalkenoate cements. *J Mater Sci Mater Med* 2006; 17: 489–494.

14. Greenspan DC, West JK, Lee S, et al. Anti-inflammatory and antimicrobial uses for bioactive glass compositions. Patent US2004228905, USA, 2004.
15. Gilchrist T and Healy DM. Antimicrobial composition composed of controlled release glasses. Patent US6143318(A), USA, 2000.
16. Wers E, Oudadesse H, Lefeuvre B, et al. Excess entropy and thermal behavior of cu-and Ti-doped bioactive glasses. *J Therm Anal Calorim* 2014; 117: 579–588.
17. Hoppe A, Güldal NS and Boccaccini AR. A review of the biological response to ionic dissolution products from bioactive glasses and glass-ceramics. *Biomaterials* 2011; 32: 2757–2774.
18. Mouriño V, Cattalini JP, Roether JA, et al. Composite polymer-bioceramic scaffolds with drug delivery capability for bone tissue engineering. *Expert Opin Drug Delivery* 2013; 10: 1353–1365.
19. Courthéoux L, Lao J, Nedelec J-M, et al. Controlled bioactivity in Zinc-doped sol-gel-derived binary bioactive glasses. *J Phys Chem C* 2008; 112: 13663–13667.
20. Fredholm YC, Karpukhina N, Brauer DS, et al. Influence of strontium for calcium substitution in bioactive glasses on degradation, ion release and apatite formation. *J R Soc Interface* 2012; 9: 880–889.
21. Murphy S, Boyd D, Moane S, et al. The effect of composition on ion release from Ca–Sr–Na–Zn–Si glass bone grafts. *J Mater Sci Mater Med* 2009; 20: 2207–2214.
22. Gerhardt L-C and Boccaccini AR. Bioactive glass and glass-ceramic scaffolds for bone tissue engineering. *Materials* 2010; 3: 3867–3910.
23. Goh Y-F, Alshemary AZ, Akram M, et al. In vitro study of nano-sized zinc doped bioactive glass. *Mater Chem Phys* 2013; 137: 1031–1038.
24. O'Donnell MD and Hill RG. Influence of strontium and the importance of glass chemistry and structure when designing bioactive glasses for bone regeneration. *Acta Biomater* 2010; 6: 2382–2385.
25. Miola M, Verné E, Vitale-Brovarone C, et al. Antibacterial bioglass-derived scaffolds: innovative synthesis approach and characterization. *Int J Appl Glass Sci* 2016; 7: 238–247.
26. Stevens MM and George JH. Exploring and engineering the cell surface interface. *Science* 2005; 310: 1135–1138.
27. Kim HW, Kim HE and Knowles JC. Production and potential of bioactive glass nanofibers as a next-generation biomaterial. *Adv Funct Mater* 2006; 16: 1529.
28. Kim HW, Lee HH and Chun GS. Bioactivity and osteoblast responses of novel biomedical nanocomposites of bioactive glass nanofiber filled poly(lactic acid). *J Biomed Mater Res Part A* 2008; 85: 651–663.
29. Poologasundarampillai G, Wang D, Li S, et al. Cotton-wool-like bioactive glasses for bone regeneration. *Acta Biomater* 2014; 10: 3733–3746.
30. Quintero F, Pou J, Comesaña R, et al. Laser spinning of bioactive glass nanofibers. *Adv Funct Mater* 2009; 19: 3084–3090.
31. Quintero F, Mann AB, Pou J, et al. Rapid production of ultralong amorphous ceramic nanofibers by laser spinning. *Appl Phys Lett* 2007; 90: 153109.
32. Cabal B, Quintero F, Díaz LA, et al. Nanocomposites of silver nanoparticles embedded in glass nanofibres obtained by laser spinning. *Nanoscale* 2013; 5: 3948–3953.
33. Wu ZY, Hill RG and Jones JR. Optimizing the processing of porous melt-derived bioactive glass scaffolds. *Bioceram Dev Appl* 2011; 1: D110150.
34. Quintero F, Comesaña R, Lusquiños F, et al. Production of zinc and strontium containing bioactive glass nanofibers. In: *24th European conference on biomaterials – annual conference of the European Society for Biomaterials*, ESB 2011; Dublin; Ireland. 4–8 September 2011.
35. Lupu AR and Popescu T. The noncellular reduction of MTT tetrazolium salt by TiO_2 nanoparticles and its implications for cytotoxicity assays. *Toxicol in Vitro* 2013; 27: 1445–1450.
36. Santhana RL, Hing HL, Baharudin O, et al. Rapid method for transmission electron microscope study of Staphylococcus aureus ATCC 25923. *Ann Microscope* 2007; 7: 102–108.
37. Doweidar H. Density-structure correlations in silicate glasses. *J Non-Cryst Solids* 1999; 249: 194–200.
38. Elgayar I, Aliev AE, Boccaccini AR, et al. Structural analysis of bioactive glasses. *J Non-Cryst Solids* 2005; 351: 173–183.
39. Oréfice RL, Hench LL, Clark AE, et al. Novel sol-gel bioactive fibers. *J Biomed Mater Res* 2001; 55: 460–467.
40. Massera J, Ahmed I, Petit L, et al. Phosphate-based glass fiber vs. bulk glass: change in fiber optical response to probe in vitro glass reactivity. *Mater Sci Eng C* 2014; 25: 251–257.
41. Hu S, Chang J, Liu M, et al. Study on antibacterial effect of 45S5 bioglass®. *J Mater Sci Mater Med* 2009; 20: 281–286.
42. Hench LL. *An introduction to bioceramics*, 2nd ed. London, UK: Imperial College Press, 2013.
43. Zhang D, Leppäranta O, Munukka E, et al. Antibacterial effects and dissolution behavior of six bioactive glasses. *J Biomed Mater Res Part A* 2010; 93: 475–483.
44. Palza H, Escobar B, Bejarano J, et al. Designing antimicrobial bioactive glass materials with embedded metal ions synthesized by the sol–gel method. *Mater Sci Eng C* 2013; 33: 3795–3801.
45. Gentleman E, Fredholm YC, Jell G, et al. The effects of strontium-substituted bioactive glasses on osteoblasts and osteoclasts in vitro. *Biomaterials* 2010; 31: 3949–3956.
46. Watts SJ, Hill RG, O'Donnell MD, et al. Influence of magnesia on the structure and properties of bioactive glasses. *J Non-Cryst Solids* 2010; 356: 517–524.
47. Misra SK, Ansari TI, Valappil SP, et al. Poly(3-hydroxybutyrate) multifunctional composite scaffolds for tissue engineering applications. *Biomaterials* 2010; 31: 2806–2815.
48. Gorriti MF, López JMP, Boccaccini AR, et al. In vitro study of the antibacterial activity of bioactive Glass-ceramic scaffolds. *Adv Eng Mater* 2009; 11: B67–B70.
49. Rivadeneira J, Carina Audisio M, Boccaccini AR, et al. In vitro antistaphylococcal effects of a novel 45S5

bioglass/agar–gelatin biocomposite films. *J Appl Microbiol* 2013; 115: 604–612.
50. Clarkin O, Wren A, Thornton R, et al. Antibacterial analysis of a zinc-based glass polyalkenoate cement. *J Biomater Appl* 2011; 26: 277–292.
51. Arakha M, Saleem M, Mallick BC, et al. The effects of interfacial potential on antimicrobial propensity of ZnO nanoparticle. *Scientific Rep* 2015; 5: 9578.
52. Ann LC, Mahmud S, Bakhori SKM, et al. Antibacterial responses of zinc oxide structures against *Staphylococcus aureus*, *Pseudomonas aeruginosa* and *Streptococcus pyogenes*. *Ceram Int* 2014; 40: 2993–3001.
53. Chudobova D, Dostalova S, Ruttkay-Nedecky B, et al. The effect of metal ions on S*taphylococcus aureus* revealed by biochemical and mass spectrometric analyses. *Microbiol Res* 2015; 170: 147–156.
54. Dutta RK, Nenavathu BP, Gangishetty MK, et al. Antibacterial effect of chronic exposure of low concentration ZnO nanoparticles on *E coli*. *J Environ Sci Health Part A Toxic/Hazard Subst Environ Eng* 2013; 48: 871–878.
55. Atmaca S, Gul K and Clcek R. The effect of zinc on microbial growth. *Turk J Med Sci* 1998; 28: 595–597.
56. Kolmas J, Groszyk E and Kwiatkowska-Rózycka D. Substituted hydroxyapatites with antibacterial properties. *BioMed Res Int* 2014; 2014: 178123.
57. Söderberg TA, Sunzel B, Holm S, et al. Antibacterial effect of zinc oxide in vitro. *Scand J Plast Reconstr Surg* 1990; 24: 193–197.
58. Kokubo T, Kim H-M and Kawashita M. Novel bioactive materials with different mechanical properties. *Biomaterials* 2003; 24: 2161–2175.
59. Vallet-Regí M, Victoria Ragel C and Salinas AJ. Glasses with medical applications. *Eur J Inorg Chem* 2003; 2003: 1029–1042.
60. Erol M, Özyuguran A and Çelebican O. Synthesis, characterization, and in vitro bioactivity of Sol-Gel-Derived Zn, Mg, and Zn-Mg co-doped bioactive glasses. *Chem Eng Technol* 2010; 33: 1066–1074.
61. Echezarreta-López MM, De Miguel T, Quintero F, et al. Antibacterial properties of laser spinning glass nanofibers. *Int J Pharm* 2014; 477: 113–121.